

Incorporating variable RBE in IMPT optimization for ependymoma

H. M. Goudarzi¹, G. Lim¹, D. Grosshans², R. Mohan², and W. Cao^{2*}

1. Department of Industrial Engineering, University of Houston

2. Department of Radiation Physics, University of Texas MD Anderson Cancer Center

Purpose: To study the dosimetric impact of incorporating variable relative biological effectiveness (RBE) of protons in optimizing intensity-modulated proton therapy (IMPT) treatment plans and to compare it with conventional constant RBE optimization and linear energy transfer (LET)-based optimization.

Methods: This study included 10 pediatric ependymoma patients with challenging anatomical features for treatment planning. Four plans were generated for each patient according to different optimization strategies: (1) constant RBE optimization (ConstRBEopt) considering standard-of-care dose requirements; (2) LET optimization (LETopt) using a composite cost function simultaneously optimizing dose-averaged LET (LET_d) and dose; (3) variable RBE optimization (VarRBEopt) using a recent phenomenological RBE model developed by McNamara et al.; (4) hybrid RBE optimization (hRBEopt) assuming constant RBE for the target and variable RBE for organs at risk. By normalizing each plan to obtain the same target coverage in either constant or variable RBE, we compared dose, LET_d , LET-weighted dose, and equivalent uniform dose between the different optimization approaches.

Results: We found that the LETopt plans consistently achieved increased LET in tumor targets and similar or decreased LET in critical organs compared to other plans. On average, the VarRBEopt plans achieved lower mean and maximum doses with both constant and variable RBE in the brainstem and spinal cord for all 10 patients. To compensate for the underdosing of targets with 1.1 RBE for the VarRBEopt plans, the hRBEopt plans achieved higher physical dose in targets and reduced mean and especially maximum variable RBE doses compared to the ConstRBEopt and LETopt plans.

27 **Conclusion:** We demonstrated the feasibility of directly incorporating variable RBE models in
28 IMPT optimization. A hybrid RBE optimization strategy showed potential for clinical
29 implementation by maintaining all current dose limits and reducing the incidence of high RBE in
30 critical normal tissues in ependymoma patients.

31

32 **1. Introduction**

33 Proton therapy has become an increasingly important treatment option for cancer patients
34 because of its dosimetical advantages over photon therapy.¹ Protons' physical characteristics
35 make it possible to generate highly conformal radiation treatment plans in which the desired dose
36 surrounds the target tightly while the dose deposited in nearby normal tissues is minimized. In the
37 current practice of proton beam therapy, prescribed doses are usually determined by scaling the
38 physical proton dose using a proton relative biological effectiveness (RBE) value of 1.1.² The
39 constant RBE value of 1.1 is based on the assumption that protons are 10% more biologically
40 effective than photons and accounts for this higher cell-killing efficiency regardless of tissue type.
41 However, in vitro and in vivo studies indicate that RBE varies within a treatment field according
42 to physical and biological factors.³ Proton therapy might be less effective if such variability is
43 ignored. Because of the assumption of constant RBE, coupled with physical uncertainties during
44 treatment delivery, the distribution of “true” biologically effective doses received by the patient
45 may differ from what is indicated on the treatment plan to an unknown, possibly significant,
46 magnitude. Consequently, unanticipated toxicities may occur and/or the patient’s disease may not
47 be controlled.⁴⁻⁷

48 While the impact of physical uncertainties involved in proton therapy, such as patient
49 setup and proton range uncertainties, may be effectively mitigated by robust optimization
50 techniques, which are increasingly being implemented in clinical practice, RBE variations and
51 appropriate treatment planning strategies are still under active investigation. RBE is known to
52 depend on particle type, linear energy transfer (LET), tissue type (α/β ratio), dose per fraction,
53 and biological endpoint, among other factors.⁸⁻¹¹ Various RBE models have been developed to
54 calculate biologically effective (RBE-weighted) dose distributions using in vitro cell survival data
55 for particles such as carbon ions and protons. The local effect model is a prominent RBE model
56 for carbon ions and has been applied clinically in carbon ion therapy.^{12,13} Although currently only

57 constant RBE is used in clinical proton therapy as the standard for dose prescription and
58 treatment planning, clinical proton centers are actively investigating the risks of RBE variations
59 and evaluating RBE-weighted dose using LET-parameterized RBE models to various extents.¹⁴
60 These models include either empirical or mechanism-based ones, which are all established by
61 applying the linear-quadratic model with radiation sensitivity parameters α and β for protons.^{15–20}
62 Frese et al. first studied the feasibility of including variable RBE in intensity-modulated proton
63 therapy (IMPT) optimization using a cost function defined by biological effect, i.e., $\alpha D + \beta D^2$
64 (D is absorbed dose and parameters α and β are for protons).^{18,21}

65 In contrast to anticipated dependence of RBE on LET among other factors, there are also
66 studies suggesting that RBE may not correlate with LET clinically.^{22,23} For example, Niemierko
67 et al. analysis on 50 brains cases suggests despite the increase in LET and RBE towards the end
68 of the range, the actual impact on patients may be relatively modest in comparison to the inherent
69 interpatient variability in radiosensitivity.²²

70 Nevertheless, current proton RBE models are still associated with substantial
71 uncertainties in biological measurement, interpretation of measured assay data, dosimetry, and
72 assumptions about simulated mechanisms. While published studies of in vitro experiments
73 indicate nonnegligible uncertainties in RBE models, they agree that RBE of protons increases
74 linearly with dose-averaged LET, and non-linearly at higher LETs near and beyond the Bragg
75 peak. This highlights the prediction that RBE climbs to significantly higher than 1.1 near the end
76 of proton beam range, where LET increases sharply. Therefore, recent research has put extensive
77 attention on incorporating LET instead of RBE into treatment planning, so that the uncertainties
78 in biophysical RBE models are avoided. In addition, LET can be accurately calculated because it
79 is entirely based on physical properties.

80 LET-based IMPT optimization can be achieved either by a two-step approach, in which
81 first physical dose is optimized and second LET is optimized with limited change to physical

82 dose,²⁴ or in a simultaneous manner using a composite cost function of both LET and dose.^{25,26}
83 Some other recent studies incorporating LET criteria include proton track-end optimization²⁷,
84 beam angle optimization²⁸, and robust optimization²⁹. The goal of LET optimization is to increase
85 LET in target regions and decrease it in normal tissues while maintaining the dose constraints (in
86 constant RBE) specified in current practice. However, the obvious drawback of LET optimization
87 is that biologically effective dose does not depend upon LET alone and, thus, increasing or
88 decreasing LET in a tumor or normal tissue would not correctly reflect its clinical consequences.

89 The main objective of the present study was two-fold. The first was to assess the impact
90 of variable RBE-weighted dose optimization on physical dose distribution compared to
91 conventional and LET optimization; the second was to investigate the efficacy of variable RBE
92 optimization in improving LET and RBE effect compared to LET optimization. We focused this
93 study on a cohort of pediatric ependymoma patients, as these cases often present critical serial
94 organs, e.g., the brainstem and spinal cord, in very close proximity to the tumorous area;
95 therefore, preventing overdosing or underdosing of biological dose is highly important. In
96 addition, we explored a variant approach of biological optimization in which variable RBE is
97 only considered for critical normal tissues to demonstrate another possible scenario in which RBE
98 models could be incorporated into treatment planning with current clinical prescription protocols.

99 It should be highlighted that our study does not aim to provide a comprehensive
100 discussion of the clinical implications of variable RBE optimization; instead, it attempts to show
101 some exploratory evidence on how variable RBE can be directly incorporated into treatment
102 planning and the dosimetric effect of doing so, via comparisons to multiple competing
103 approaches.

104

105 2. Materials and Methods

106 In this study, four IMPT plan optimization approaches, constant RBE optimization
 107 (ConstRBEopt), LET-based optimization (LETopt), variable RBE optimization (VarRBEopt),
 108 and hybrid RBE optimization (hRBEopt), were implemented and compared. While variable RBE
 109 weighted dose was calculated for optimization in VarRBEopt and hRBEopt, only constant RBE
 110 weighted dose was used in LETopt and ConstRBEopt, for plan generation. However, both
 111 variable and constant RBE weighted doses for all four plans were calculated for plan evaluation.

112 The physical dose D_i and dose-averaged LET (LET_d) L_i are calculated as follows:

$$113 \quad D_i = \sum_j D_{ij} w_j, \quad (1)$$

$$114 \quad L_i = \frac{\sum_j D_{ij} L_{ij} w_j}{\sum_j D_{ij} w_j}, \quad (2)$$

115 where D_{ij} and L_{ij} are the dose and LET contributions from beamlet j to voxel i in unit intensity,
 116 respectively, and w_j indicates the intensity of beamlet j .

117 The cost function for the ConstRBEopt, VarRBEopt, and hRBEopt models a sum of
 118 quadratic terms penalizing deviations between achieved and prescribed doses, as demonstrated in
 119 equation (3).

$$120 \quad F_D(w) = \sum_{i=1}^{N_T} \frac{\lambda_T^+}{|N_T|} (RBE_i \cdot D_{i \in T} - D_{i \in T}^{pr})_+^2 + \sum_{i=1}^{N_T} \frac{\lambda_T^-}{|N_T|} (RBE_i \cdot D_{i \in T} - D_{i \in T}^{pr})_-^2$$

$$121 \quad + \sum_{i=1}^{N_O} \frac{\lambda_O^+}{|N_O|} (RBE_i \cdot D_{i \in O} - D_{i \in O}^{pr})_+^2 \quad (3)$$

122 In (3), $D_{i \in T}^{pr}$ and $D_{i \in O}^{pr}$ demonstrate the prescribed dose in Gy(RBE) for tumor and organs at risk
 123 (OARs), respectively; λ_T^+ and λ_T^- are penalty weighting factors for overdosing and underdosing the
 124 target, respectively; λ_O^+ is for normal tissue overdosing; N_T and N_O are the numbers of target and

125 OAR voxels, respectively. For ConstRBEopt, RBE_i is set to 1.1 for all voxels. For VarRBEopt,
 126 RBE_i is calculated using the model described by McNamara et al.¹⁵ For hRBEopt, RBE_i is constant
 127 1.1 for target voxels and variable (also using the McNamara model) for OAR voxels. When target
 128 and OARs overlap, constant RBE is used for those overlapping voxels.

129 The RBE model introduced by McNamara et al.¹⁵ is shown in equation (4). We consider two tissue-
 130 specific parameters, i.e., $(\alpha/\beta)_x = 2$ for OARs (brainstem and spinal cord) and $(\alpha/\beta)_x = 10$ for
 131 tumor, in this study.

$$132 \quad RBE \left[D_P, \frac{\alpha}{\beta}, LET_d \right] =$$

$$133 \quad \frac{1}{2D_P} \left(\sqrt{\left(\frac{\alpha}{\beta} \right)_x^2 + 4D_P \left(\frac{\alpha}{\beta} \right)_x \left(0.999064 + \frac{0.35605}{\left(\frac{\alpha}{\beta} \right)_x} LET_d \right) + 4D_P^2 \left(1.1012 - 0.0038703 \sqrt{\left(\frac{\alpha}{\beta} \right)_x} LET_d \right)^2} \right.$$

$$134 \quad \left. - \left(\frac{\alpha}{\beta} \right)_x \right) \quad (4)$$

135 The cost function for LETopt (5) is formulated by adding two quadratic terms,
 136 maximizing LET in target and minimizing LET in OARs, to the dose-only cost function (3). The
 137 goal of this cost function is to optimize dose and LET distributions simultaneously.

$$138 \quad F_L(w) = F_D(w) - \frac{\gamma_T}{|N_T|} \sum_{i=1}^{N_T} L_{i \in T}^2 + \frac{\gamma_O}{|N_O|} \sum_{i=1}^{N_O} L_{i \in O}^2 \quad (5)$$

139 In (5), γ_T and γ_O are weighting factors to control the priorities of LET in target and OARs,
 140 respectively.

141 We used matRad³⁰, an open-source treatment planning system for radiation therapy
 142 written in Matlab, to create all IMPT plans and produce dose and LET influence matrices. The

143 voxel size was set to $3 \times 3 \times 3 \text{ mm}^3$. The lateral spot spacing was 5 mm, and the energy layers
 144 were interpolated uniformly with a spacing of 2 mm in the beam direction. Analytical models
 145 were used in matRad for calculating dose³¹ and LET³². The accuracy of the models was validated
 146 by Monte Carlo calculations in previous studies.^{32,33} All the IMPT optimization problems
 147 mentioned in this paper are highly non-convex. Hence, we solved those problems using the
 148 Interior Point Optimizer (IPOPT)³⁴, a solver developed for large-scale nonlinear optimization
 149 instances and also included in matRad. All computations were performed on a laptop with an
 150 Intel Core i7 CPU (3.6 GHz) and 12 GB of RAM.

151 For all 10 pediatric ependymoma cases, a dose prescription of 54 Gy(RBE) (RBE-
 152 weighted dose) was prescribed for delivery in 30 fractions to the clinical target volume (CTV).
 153 The OARs considered were brainstem and spinal cord for all patients. The maximum voxel dose
 154 constraints were 50 Gy(RBE) for the spinal cord and 57 Gy(RBE) for the brainstem. Note that we
 155 considered variable RBE weighted dose for all dose constraints (target and OARs) for
 156 VarRBEopt, and constant RBE weighted dose for LETopt and ConstRBEopt, whereas hRBEopt
 157 used constant RBE for target constraints and variable RBE for OAR constraints. The CTV was
 158 set as the optimization target. Here, all plans utilized the clinically used treatment field angles for
 159 each patient. Details of the beam angles, number of voxels, and number of beamlets for each
 160 patient are shown in Table 1.

161

162 Table 1. Patient information and key treatment planning parameters.

Case #	Beam angles (Gantry, Couch)	Number of beamlets	Total number of voxels (Target, Brainstem, Spinal Cord)	Number of overlapping voxels (Target \cap Brainstem)
1	(100,12), (260,348), (280,45), (80,315)	1248	1100 (661, 385, 54)	88
2	(180,0), (270,15), (90,345)	2578	2047 (1529, 391, 127)	116

3	(245,0), (180,0), (112,0), (315,0)	2044	2099 (907, 719, 473)	87
4	(60,0), (260,15), (305,0), (160,0)	5313	3365 (2688, 372, 305)	284
5	(290,345), (70,15)	1261	2121 (1230, 805, 86)	0
6	(155,0), (75,0), (310,0), (205,0)	1374	1316 (695, 362, 259)	59
7	(325,0), (252,20), (175,0), (100,0)	2001	1482 (995, 436, 51)	27
8	(105,0), (255,0), (285,90)	1018	1514 (680, 739, 95)	75
9	(290,90), (270,0), (90,0)	1110	2229 (801, 1043, 385)	169
10	(290,90), (270,0), (90,0), (180,0)	2096	1854 (1014, 657, 183)	52

163

164 It should be mentioned that each of the four plans per patient was optimized
165 independently, with a starting condition of uniform beamlet intensity. No base plan was used to
166 create the LETopt, VarRBEopt and hRBEopt plans. Furthermore, in plan generation, each plan
167 was normalized to meet the same target coverage, i.e., 90% of the CTV covered by the prescribed
168 dose, after optimization. Note that the plan normalization in this study was based on RBE
169 weighted dose with different RBE schemes according to different plans. In other words, the
170 VarRBEopt plan was normalized so that the variable RBE weighted dose reaches the target
171 coverage benchmark, but the other three plans used constant RBE-weighted dose for
172 normalization. In plan evaluation, all plans were re-calculated using both constant and variable
173 RBE. For comparison purposes, the VarRBEopt plans were also re-normalized so that constant
174 RBE weighted dose could meet the target coverage benchmark. The choice of using 90% target
175 coverage of prescription dose as the normalization benchmark is based on our experience in
176 planning these patients for original IMPT treatments in the clinic. Most patients present complex
177 concave tumor shapes and considerable proximity or overlap between target volume and
178 brainstem. We found 90% target coverage (lower than typical clinical protocols) is a reasonable

179 threshold to balance the need to meet the critical organ dose limit (protecting brainstem and
180 spinal cord as top priority for pediatric patients) and increase target dose as much as possible³⁵.

181 To study the effects of the different optimization strategies, various dosimetric measures
182 were evaluated, including distributions of doses recalculated in both constant and variable RBE,
183 dose-volume histograms (DVHs), dose-averaged LET (LET_d), LET-volume histograms (LEV-
184 VHs), maximum (and mean) dose and LET_d to a voxel, as well as generalized equivalent uniform
185 dose (gEUD).^{36,37} We also included analysis of LET-weighted dose ($c \text{ LET} \times D$), a metric
186 embraced in many recent studies^{24,28,29,38,39}. If biological dose or RBE-weighted dose is defined
187 by a simple LET parameterized form: $D + c \text{ LET} \times D$, the product of LET and physical dose D
188 (i.e., LET-weighted dose), can be seen as an extra component of LET effect in total biological
189 dose, which “models” the linear increase of RBE with LET. For single dosimetric indices per
190 structure, such as mean and maximum dose or LET, we used paired t-test to determine if the
191 mean difference between two treatment plans is significantly different than 0, or if the average is
192 significantly different. A confidence level of 95% was chosen for hypothesis testing and p-value
193 ≤ 0.05 was considered statistically significant for a particular plan quality index in a two-plan
194 comparison.

195 In addition, we introduced and exploited the differential EUD concept to evaluate the
196 differential gain of biological based optimization compared to conventional optimization. The
197 differential EUD quantifies the EUD difference between a test plan TP (e.g., a
198 LET/VarRBE/hRBE optimization plan) and a reference plan RP (e.g., a ConstRBE optimization
199 plan) for a given volume of interest (VOI), i.e., ΔEUD_{VOI} as defined by equation (6). The sum of
200 differential EUD can present a single composite score comparing two plans by including multiple
201 VOIs (target volumes and normal tissues), i.e., ΔEUD as defined by the linear equation (7).

$$202 \quad \Delta EUD_{VOI}(TP - RP) = EUD_{VOI}(TP) - EUD_{VOI}(RP) \quad (6)$$

$$\Delta EUD = \sum_k \gamma_{T_k} \times \Delta EUD_{T_k} - \sum_k \gamma_{N_k} \times \Delta EUD_{N_k} \quad (7)$$

When computing ΔEUD , γ_{T_k} and γ_{N_k} are user-defined parameters to balance the priority of each of the target volumes and normal tissues in a specific evaluation. We used equal weights ($\gamma_{T_k} = 1, \gamma_{N_k} = 1$) in this study.

Here the organ specific EUD is defined by generalized EUD (gEUD) in this study.^{36,37}

The gEUD for each VOI is calculated by the following formula,

$$gEUD = (\sum_i v_i D_i^a)^{\frac{1}{a}}, \quad (8)$$

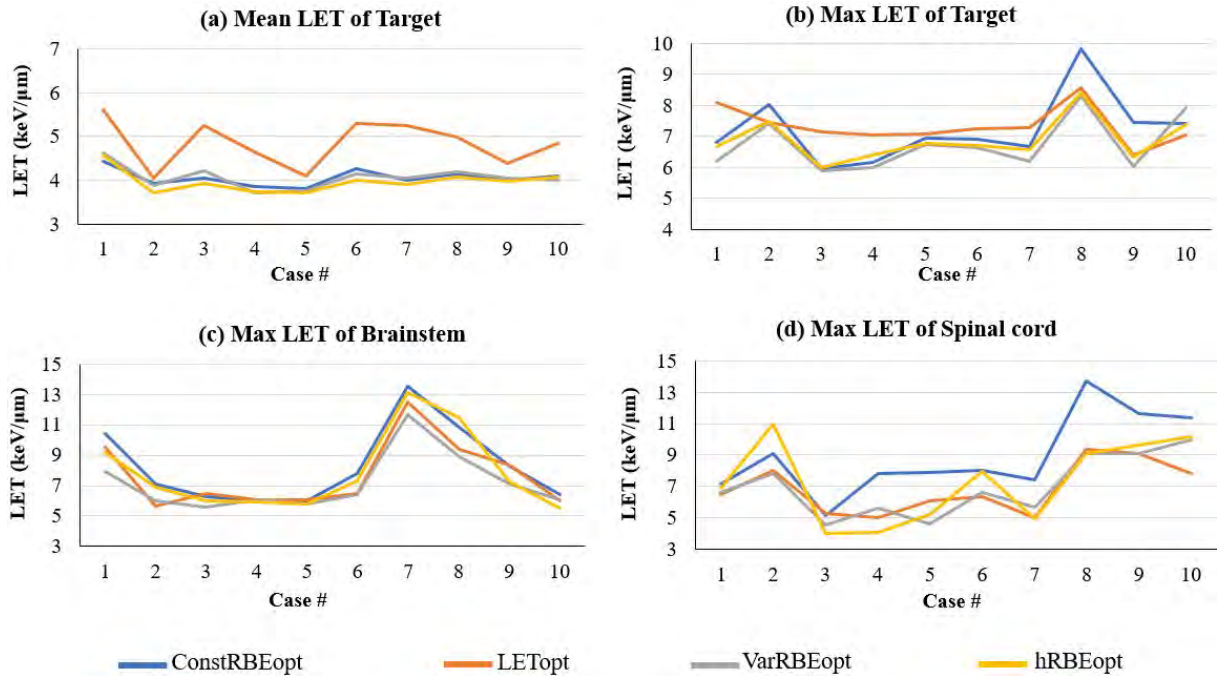
where v_i is representing the fractional organ volume receiving a dose D_i , and a is a tissue-specific parameter that characterizes the volume effect and varies according to the tissue type. In gEUD calculation, we chose a value of -10 for the parameter a for the target to mimic the effect of cold spots on tumor control probability and 10 for the brainstem and spinal cord to reflect the dependence of highest dose in the tissue for serial organs.⁴⁰⁻⁴² We should note that ΔEUD can be measured for either variable or constant RBE-weighted dose distributions. A positive value of ΔEUD in the present definition indicates a gain in EUD for the test plan over the reference plan. For a specific VOI, a positive value of ΔEUD_{VOI} simply means higher EUD of the test plan than the reference plan.

219

220 3. Results

The mean and max LET of the target and max LET of the brainstem and spinal cord obtained from each plan are shown in Figure 1, respectively. On average, LETopt led to a marked increase of mean LET in the target by 19%, 19%, and 22% compared to ConstRBEopt, VarRBEopt, and hRBEopt, respectively ($p < 0.001$ for all), for the 10 ependymoma patients. However, there was no statistically significant difference in max LET in the brainstem between

226 LET_{opt} and VarRBE_{opt} or hRBE_{opt} ($p > 0.05$ for both). For the spinal cord, reductions in max
 227 LET by LET_{opt} and VarRBE_{opt} compared to ConstRBE_{opt} were statistically significant ($p <$
 228 0.001 for both). Meanwhile, no statistically significant difference was found between LET_{opt},
 229 VarRBE_{opt} and hRBE_{opt} plans in terms of spinal cord max LET ($p > 0.05$ for all). Detailed
 230 values of LET for all plans are listed in Appendix (Tables 1-3).

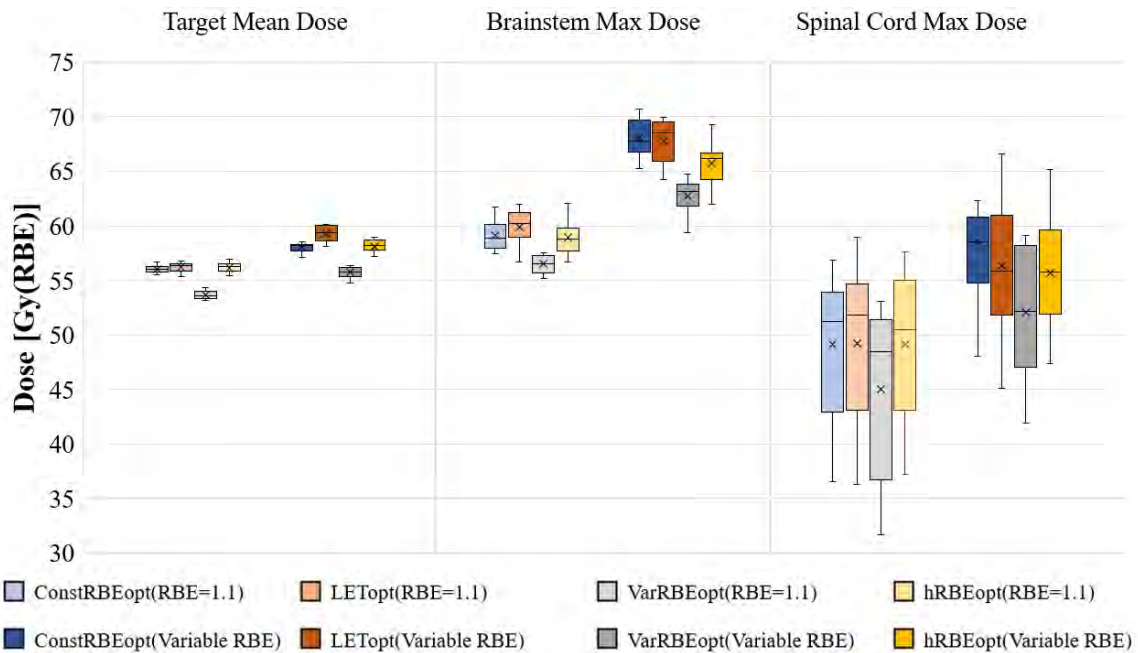


231
 232 Figure 1. Mean (a) and max (b) LET for target, max LET for brainstem (c) and spinal cord (d)
 233 from ConstRBE_{opt}, LET_{opt}, VarRBE_{opt}, and hRBE_{opt} plans for 10 ependymoma cases.

234

235 Figure 2 summarizes the target mean dose, brainstem max dose, and spinal cord max
 236 dose (maximum dose of all voxels in spinal cord) based on both constant and variable RBE for
 237 the four plans for all 10 cases. LET_{opt} increased mean variable RBE dose in the target by the
 238 most among the four optimization approaches (indicating the impact of increased LET on
 239 variable RBE-weighted dose). The VarRBE_{opt} plans achieved the lowest max dose in the
 240 brainstem and spinal cord among the plans with either constant or variable RBE. With constant

241 RBE, the average of mean doses in the brainstem obtained from VarRBEopt plan was
 242 significantly lower than the ConstRBEopt, LETopt, and hRBEopt plans, respectively ($p < 0.01$
 243 for all); but no significant difference for the spinal cord ($p > 0.05$ for all). With variable RBE,
 244 there were no significant difference in the brainstem and spinal cord mean doses either ($p > 0.05$
 245 for all). The hRBEopt plans resulted in similar max dose in the brainstem and spinal cord
 246 compared to the ConstRBEopt plan and the LETopt plan with constant RBE ($p > 0.05$ for all,
 247 except hRBEopt vs. LETopt for brainstem); however, it outperformed those two plans with
 248 variable RBE ($p < 0.05$ for all, except hRBEopt vs. LETopt for spinal cord). Also, large
 249 variations of max doses in the spinal cord were observed among the 10 patient plans. As the
 250 VarRBEopt plans were optimized to achieve required target coverage according to variable RBE,
 251 it appears that their target coverage with RBE of 1.1, for instance target $D_{90\%}$ with a mean of 51
 252 Gy(RBE) and ranging from 49.9 to 52.1 Gy(RBE), was lower than that of the other three plans
 253 (mean of 54 Gy(RBE)).

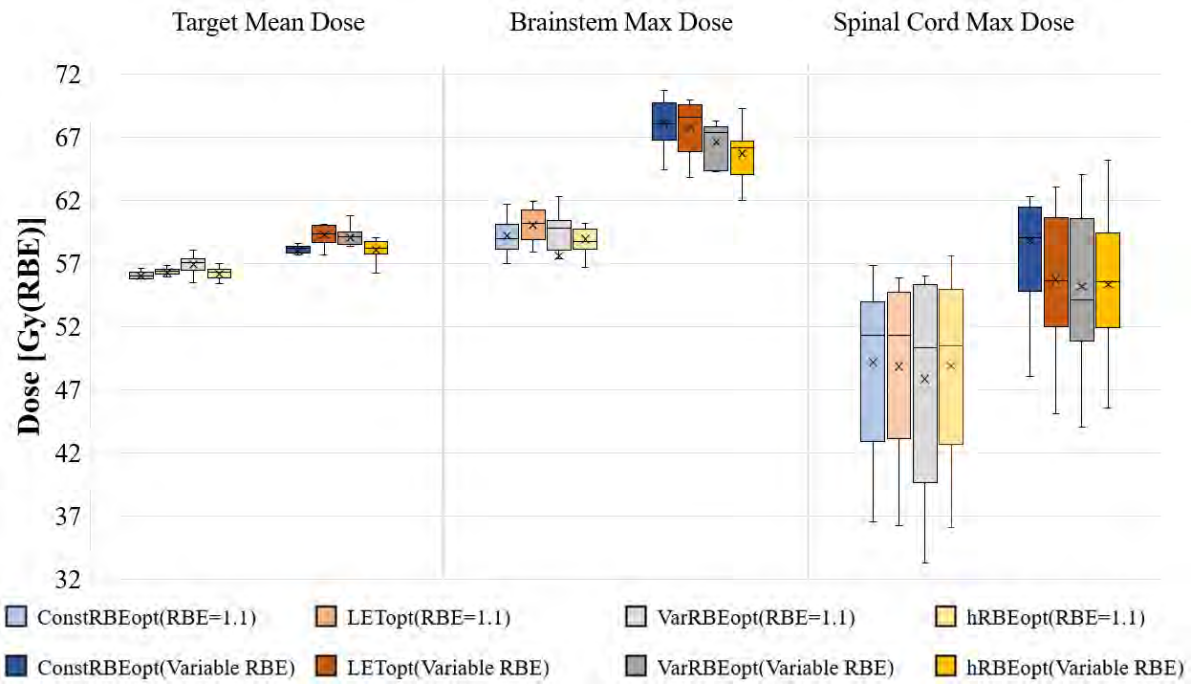


255 Figure 2. Box plot of mean dose in target, max dose in brainstem, and max dose in spinal cord of
 256 ConstRBEopt, LETopt, VarRBEopt and hRBEopt plans recalculated with constant and variable

257 RBE-weighted doses for 10 ependymoma cases. All plans were normalized to have the same
 258 target coverage for the ConstRBEopt, LETopt, hRBEopt plans in terms of 1.1 RBE and the
 259 VarRBEopt plans in terms of variable RBE.

260

261 When considering the normalization of all plans to achieve the same target coverage in
 262 1.1 RBE, as illustrated in Figure 3, the hRBEopt plans exhibited comparable target doses but
 263 displayed a significant reduction in brainstem doses compared to the ConstRBEopt plans in terms
 264 of variable RBE.

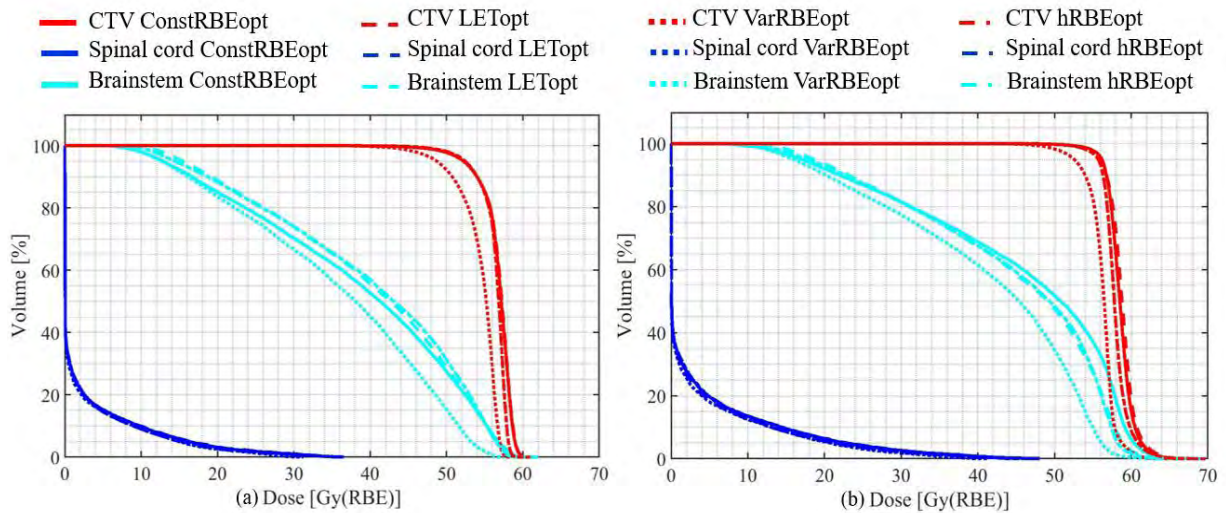


265

266 Figure 3. Box plot of mean dose in target, max dose in brainstem, and max dose in spinal cord of
 267 ConstRBEopt, LETopt, VarRBEopt and hRBEopt plans recalculated with constant and variable
 268 RBE-weighted doses for 10 ependymoma cases. All plans were normalized to have the same
 269 target coverage in terms of 1.1 RBE.

270 We also calculated differential EUDs, (6) and (7), based on variable RBE weighted dose
 271 for each of the biologically optimized plans compared to the ConstRBEopt plan (see Table 10 in
 272 Appendix). Note that positive values of ΔEUD indicate superiority of the biologically optimized
 273 plans compared to the ConstRBEopt plan and vice versa. The average [range] composite gain of
 274 LETopt, VarRBEopt, and hRBEopt with variable RBE-weighted dose over ConstRBEopt was 2.5
 275 [0.08, 6.51] Gy(RBE), 4.3 [0.07, 9.89] Gy(RBE), and 2.7 [0.18, 6.26] Gy(RBE), respectively,
 276 among the 10 ependymoma cases.

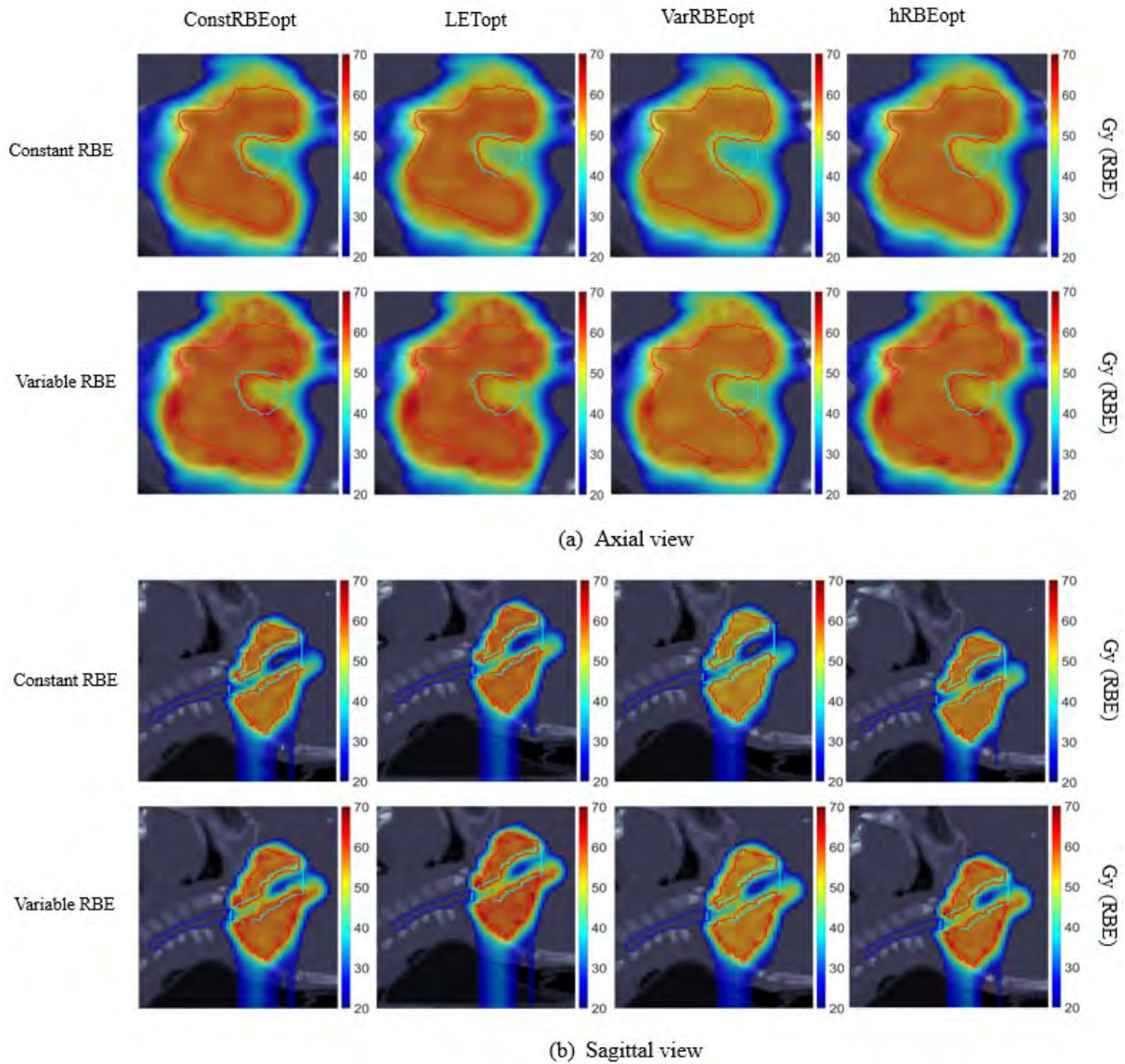
277 Figure 4 shows DVHs of all plans based on constant and variable RBE-weighted doses
 278 for an example of the 10 ependymoma cases (case #2). In both scenarios, brainstem was better
 279 spared, especially in the high-dose region, in the VarRBEopt plan than in the ConstRBEopt,
 280 LETopt, and hRBEopt plans. There was no marked difference in spinal cord DVHs among the
 281 plans. As shown in the constant RBE DVHs (Figure 4a), the $D_{90\%}$ was near 51 Gy(RBE) for the
 282 VarRBEopt plan, while all other plans had the same $D_{90\%}$ of 54 Gy(RBE).



283

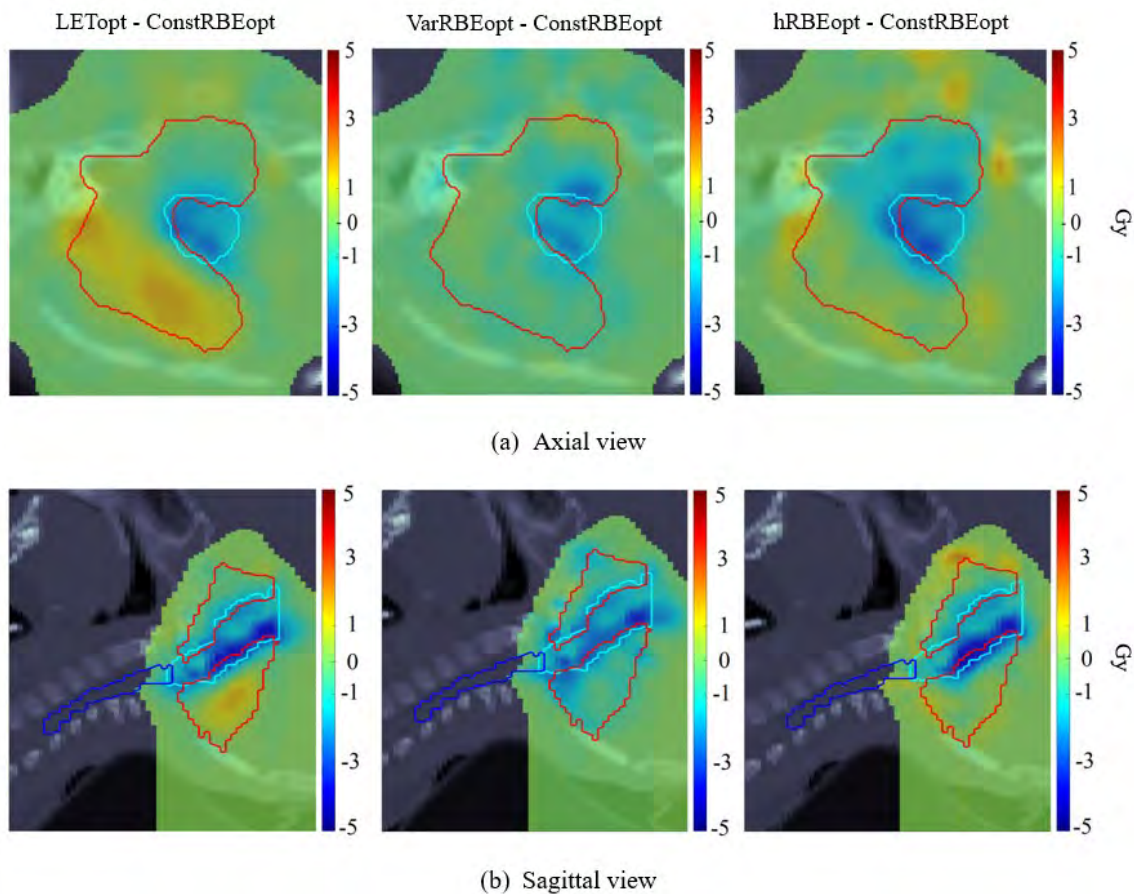
284 Figure 4. DVHs based of (a) constant and (b) variable RBE for all plans for an example
 285 ependymoma case (case #2)

286 Dose distributions in both constant and variable RBE of all four plans have been
287 reviewed. While dose within the brainstem increased when changing from constant to variable
288 RBE for all plans, the increase was most significant for the ConstRBEopt plan (example case #2
289 shown in Figure 5).



290
291 Figure 5. Axial and sagittal views of dose distributions obtained from the ConstRBEopt, LETopt,
292 VarRBEopt, and hRBEopt plans for an example ependymoma case (case #2). Red contours are
293 CTV, cyan contours are brainstem, and dark blue contours are spinal cord. Color bars represent
294 doses in Gy(RBE).

295 When evaluating the LET-weighted dose ($c \text{ LET} \times D$), each of the three biologically
 296 optimized plans showed lower LET-weighted dose in the brainstem compared to the
 297 ConstRBEopt plan. In addition, the hRBEopt plan showed greater reduction of LET-weighted
 298 dose in the brainstem than did the LETopt and VarRBEopt plans, although this was at the
 299 expense of a relatively cooler CTV (see example in Figure 6).



300

301 Figure 6. Axial and sagittal views of distribution showing difference in $c \text{ LET} \times D$ ($c = 0.04$
 302 $\mu\text{m}/\text{keV}$) obtained from the LETopt, VarRBEopt, and hRBEopt plans compared to the
 303 ConstRBEopt plan for an example ependymoma case (case #2). Red contours are CTV, cyan
 304 contours are brainstem, and dark blue contours are spinal cord. Color bars represent doses in Gy.

305

306 **4. Discussion**

307 As many aspects of the clinical use of proton therapy progress rapidly, including the
308 transition from passive scattering to scanning pencil beams in existing and new centers and
309 reduced planning target margins thanks to uncertainty mitigation measures, the use of a constant
310 RBE throughout the entire irradiated volume could become more problematic. Therefore,
311 improvement in understanding spatial RBE variation is increasingly critical. Although current
312 treatment planning and dose prescriptions are still based on constant RBE, some proton centers
313 have begun building capacities to assess, and even optimize, biologically effective dose (for
314 variable RBE) or surrogates for evaluation purposes in order to assist oncologists in making
315 clinical decisions.

316 Research on treatment plan optimization using variable RBE models is currently limited.
317 Variable RBE was first incorporated into IMPT plan optimization by Frese et al.¹⁸ using a cost
318 function of biological effect. Recently, Hahn et al.⁴³ reported another approach in which both
319 constant and variable RBE weighted doses are included in the cost function. So far, most studies
320 of biologically based IMPT planning have focused on LET or LET-weighted dose optimization
321 ^{24–29,38,44}. Our study aimed to compare the effectiveness of RBE and LET optimization approaches
322 for tailoring RBE and LET distributions.

323 As found in previous studies^{17,45}, we demonstrated that IMPT plan optimization using
324 variable RBE models can obtain comparable dosimetric quality in the domain of constant RBE
325 while reducing variable RBE-weighted dose in critical normal structures compared to
326 conventional constant RBE optimization. Note that these three studies (including this one) were
327 based on three different empirical RBE models. The Frese study used the Wilkens and Oelfke
328 model⁴⁶, in which the proton tissue parameter β is independent of LET. The Hahn study used the
329 Wedenberg model¹⁶, in which proton β increases with increasing LET. The McNamara model¹⁵
330 used in the present study used a similar form of the Wedenberg model, but its parameters were

331 fitted from more comprehensive experimental cell survival data. It is likely that the differential
332 impact between variable and constant RBE optimization depends on the RBE model chosen.
333 However, it is reasonable to conjecture that the trend of reducing high RBE in normal structures
334 would be consistent across models. Additional research is needed to support such insight. One
335 example is from a recent study by Giovannini et al.⁴⁷, which gave a thorough comparison of three
336 RBE models: Carabe⁴⁸, Wedenberg¹⁶, and local effect model⁴⁹.

337 Because it employs an RBE value higher than 1.1, VarRBEopt resulted in a lower
338 physical dose in the target (about 2.5 Gy(RBE) in mean dose) and/or OARs (about 2.3 Gy(RBE)
339 in mean dose) compared to other approaches in our study. Similar results were observed in other
340 studies^{17,45}. Thus, the VarRBEopt plans could not be approved clinically if a target dose
341 prescription in RBE of 1.1 must be satisfied (see example in Figure 4). To remedy this scenario
342 for immediate clinical applications of variable RBE optimization, one could use a hybrid
343 approach (hRBEopt) to enforce target dose criteria with RBE of 1.1 while using a variable RBE
344 model for OAR criteria. Although the hRBEopt plans compromised on OAR sparing - reduced
345 physical and variable RBE dose, as achieved by VarRBEopt, these plans were still more
346 advantageous than the ConstRBEopt and LETopt plans in our study. Brainstem mean and max
347 dose reductions by the hRBEopt plans were 1.3 and 2.4 Gy(RBE) compared to the ConstRBEopt
348 plans, and 2.0 and 2.0 Gy(RBE) compared to the LETopt plans, respectively, on average for the
349 10 ependymoma cases. Based on a pairwise *t*-test with significance level 0.05, although mean
350 dose reduction in brainstem is not statistically significant, the max dose reduction in brainstem of
351 hRBEopt is significant compared to ConstRBEopt and LETopt with *P*-value 0.005 and 0.04. For
352 the spinal cord, the corresponding reductions were 0.3 and 3.2 Gy(RBE) compared to the
353 ConstRBEopt plans, and 0.05 and 0.4 Gy(RBE) compared to the LETopt plans. Even though the
354 average dose reduction in the spinal cord is not statistically significant when comparing hRBEopt
355 with ConstRBEopt and LETopt, there is a significant decrease in the maximum dose in the spinal

356 cord in hRBEopt compared to ConstRBEopt with P -value of 0.01. In another example, if all plans
357 are normalized to have the same target coverage in 1.1 RBE, as shown in Figure 3, the hRBEopt
358 plans achieved similar dose in target but significantly reduced dose in brainstem in variable RBE
359 compared to the ConstRBEopt plans.

360 It is worth noting that some of the plans appear to exceed the typical maximum dose
361 limits for brainstem (e.g., $D_{max} < 57 \text{ Gy(RBE)}$) or spinal cord (e.g., $D_{max} < 50 \text{ Gy(RBE)}$). It is
362 even more so for variable RBE weighted dose (Figure 2 & 3). This is mainly because the
363 normalization of each original plans to meet the same target coverage threshold for plan
364 comparison purposes and the effect of variable RBE. We should emphasize that, based on our
365 data (normalized dose distributions) in this study, biologically optimized plans could consistently
366 achieve lower RBE dose to OARs like brainstem and spinal cord, with the same target coverage,
367 compared to conventionally optimized plans. If such biological optimization approaches were
368 used in clinical practice, especially for challenging cases with overlap between target volume and
369 critical organs as seen in this study, biologically optimized plans could still be superior than the
370 conventional plans dosimetrically.

371 In the present study, LET optimization was effective in increasing LET_d in target (19%
372 increase of mean LET_d in CTV on average compared to the ConstRBEopt plans) and decreasing
373 LET in OARs (17% decrease of mean LET in brainstem) in the present study (Appendix Table 1-
374 3). The effect of LET optimization on LET_d was consistently greater than that of VarRBEopt and
375 hRBEopt. We also found that the LETopt plans increased the variable RBE-weighted dose in
376 CTV by 1.25 Gy(RBE) on average compared to the ConstRBEopt plans because of the increased
377 LET_d . However, the advantage of LETopt for enhancing biological dose in CTV may be achieved
378 at a cost of increased physical dose in the brainstem (Figure 2). Nevertheless, the maximum
379 biological doses in the brainstem for the LETopt plans were not higher than the ConstRBEopt

380 plans, due to lowered brainstem LET by LET_{opt} (Appendix – Table 2). The difference in variable
381 RBE weighted dose between these two sets of plans was not statistically significant ($p = 0.7$).

382 Although it is not trivial to obtain an accurate value for parameter c to predict RBE, c
383 $\text{LET} \times D$ could be a useful measure in biological evaluation, especially for plan comparison. In
384 this study, the VarRBE_{opt} and hRBE_{opt} plans were more effective in reducing $c \text{LET} \times D$ in
385 brainstem than was the ConstRBE_{opt} plan for our example case (Appendix – Figure 2), even
386 though they were optimized using a more complex RBE model. It is interesting that hRBE_{opt}
387 resulted in lower biological dose in some CTV voxels near the brainstem compared to the
388 ConstRBE_{opt} plan, especially because the physical or constant RBE doses were nearly the same
389 for the two plans (Appendix – Table 4). In evaluation and optimization of LET or LET-weighted
390 dose, most studies did not use a prescribed limit to these values. For example, any LET or LET-
391 weighted dose greater than zero were minimized in normal tissues. The most recent study by
392 Hahn et al.⁴³ suggested a threshold of 40 Gy(RBE) for LET optimization for cranial IMPT plans
393 based on analyzing image change (after proton therapy) data.

394 EUD could be another useful measure for biological evaluation of IMPT plans. With
395 increasing numbers of planning strategies and RBE models to be evaluated, EUD and differential
396 EUD (ΔEUD) can give planners a single composite index representing differences in plan quality.
397 In the present study, all LET_{opt}, VarRBE_{opt} and hRBE_{opt} plans were found preferable than
398 ConstRBE plans in various degrees according to a range of positive ΔEUD (in variable RBE)
399 values among different plans and patients (Appendix - Table 10). When evaluating ΔEUD per
400 VOI, i.e., $\Delta\text{EUD}_{\text{VOI}}$, higher EUDs of CTV were consistently achieved in the LET_{opt} plans,
401 compared to the ConstRBE_{opt} plans. For the VarRBE_{opt} plans, although EUDs of CTV were not
402 as high as those of the ConstRBE_{opt} plans, EUDs of brainstem and spinal cord were mostly
403 lower than for the ConstRBE_{opt} plans, which resulted in positive overall ΔEUD s for all the cases.
404 For the hRBE_{opt} plans, positive ΔEUD s were mainly attributable to lower EUDs of brainstem

405 and spinal cord compared to the ConstRBEopt plans. In addition, with constant RBE, the Δ EUDs
406 comparing LETopt, VarRBEopt, and hRBEopt with ConstRBEopt, respectively, were less than 1
407 Gy on average for all cases (Appendix - Table 11).

408 Despite the dosimetric advantages of the hybrid RBE optimization approach (hRBEopt)
409 showed in our study, clinical implementation of such strategy could be controversial, as there is
410 no clinical evidence that the RBE would be constant in tumor but variable in normal tissues in a
411 patient. While the ultimate solution in proton planning remains using variable RBE as accurately
412 as possible throughout the patient's body, the hybrid approach can provide an effective alternative
413 to reduce variable RBE-weighted dose in critical serial organs. Similar findings were reported in
414 other recent studies⁴³.

415 Regarding computational time, VarRBEopt took about 55% longer on average to solve
416 than did ConstRBEopt because of its higher complexity in calculating the gradient of its objective
417 function and more iterations to converge. Solving hRBEopt and LETopt took 39% and 10%
418 more time than ConstRBEopt, respectively. All plans took less than 6 minutes for optimization,
419 including time used for calculating dose and LET influence matrices.

420 One limitation of the present study is that robust optimization was not incorporated in the
421 tested planning approaches. It has been suggested that robust optimization (against physical
422 uncertainties) might reduce the impact of variable RBE^{50,51}. Variable RBE optimization is
423 particularly suitable for existing robust optimization methods developed for IMPT planning. One
424 only needs to replace constant RBE with variable RBE in the optimization criteria. Nevertheless,
425 incorporation of physical uncertainties into optimization of biological dose requires additional
426 investigations. Another future step to further exploit the biological effect of protons could be
427 beam angle optimization. It is likely that use of more—or nonintuitive—beam angles could lead
428 to improved biological dose distribution with added degrees of freedom in optimization. A more

429 challenging question requiring thorough study is how many more angles would be truly
430 beneficial, as in the emerging proton arc therapy.^{52,53}

431

432 **5. Conclusion**

433 In our study of variable RBE and LET effect of protons in 10 anatomically challenging
434 ependymoma cases, biologically based optimization approaches consistently outperformed
435 standard optimization using a constant RBE for IMPT treatment planning. While directly
436 optimizing variable RBE-weighted dose can achieve substantial benefit in sparing critical organs
437 like the brainstem compared to constant RBE or LET optimization approaches, it may lead to
438 target underdosing with the current standard of 1.1 RBE. With a hybrid approach of assuming
439 constant RBE for target and variable RBE for normal tissues, the benefit of variable RBE
440 optimization for brainstem protection can still exceed that of other approaches including LET
441 optimization.

442

443 **4. References**

- 444 1. Mohan R, Grosshans D. Proton therapy-present and future. *Adv Drug Deliv Rev*.
445 Published online 2016. doi:10.1016/j.addr.2016.11.006
- 446 2. Paganetti H. Proton relative biological effectiveness-uncertainties and opportunities. *Int J*
447 *Part Ther*. 2019;5(1):2-14. doi:10.14338/IJPT-18-00011.1
- 448 3. Paganetti H, Niemierko A, Ancukiewicz M, et al. Relative biological effectiveness (RBE)
449 values for proton beam therapy. *Int J Radiat Oncol Biol Phys*. 2002;53(2):407-421.
450 doi:10.1016/S0360-3016(02)02754-2
- 451 4. Mohan R, Peeler CR, Guan F, Bronk L, Cao W, Grosshans DR. Radiobiological issues in
452 proton therapy. *Acta Oncol (Madr)*. 2017;56(11):1367-1373.
453 doi:10.1080/0284186X.2017.1348621
- 454 5. Devine CA, Liu KX, Ioakeim-Ioannidou M, et al. Brainstem injury in pediatric patients
455 receiving posterior fossa photon radiation. *Int J Radiat Oncol Biol Phys*.
456 2019;105(5):1034-1042. doi:10.1016/j.ijrobp.2019.08.039
- 457 6. Underwood TSA, Grassberger C, Bass R, et al. Asymptomatic late-phase radiographic
458 changes among chest-wall patients are associated with a proton RBE exceeding 1.1. *Int J*
459 *Radiat Oncol Biol Phys*. 2018;101(4):809-819. doi:10.1016/j.ijrobp.2018.03.037
- 460 7. Peeler CR, Mirkovic D, Titt U, et al. Clinical evidence of variable proton biological
461 effectiveness in pediatric patients treated for ependymoma. *Radiother Oncol*.
462 2016;121(3):395-401. doi:10.1016/j.radonc.2016.11.001
- 463 8. Paganetti H, Luijk P Van. Biological considerations when comparing proton therapy with
464 photon therapy. *YSRAO*. 2013;23(2):77-87. doi:10.1016/j.semradonc.2012.11.002
- 465 9. Paganetti H. Relative biological effectiveness (RBE) values for proton beam therapy.

- 466 Variations as a function of biological endpoint, dose, and linear energy transfer. *Phys Med*
467 *Biol.* 2014;59(22):R419-R472. doi:10.1088/0031-9155/59/22/R419
- 468 10. Calugaru V, Nauraye C, Noël G, Giocanti N, Favaudon V, Mégnin-Chanet F.
469 Radiobiological characterization of two therapeutic proton beams with different initial
470 energy spectra used at the Institut Curie Proton Therapy Center in Orsay. *Int J Radiat*
471 *Oncol Biol Phys.* 2011;81(4):1136-1143. doi:10.1016/j.ijrobp.2010.09.003
- 472 11. Vitti ET, Parsons JL. The radiobiological effects of proton beam therapy: Impact on DNA
473 damage and repair. *Cancers (Basel).* 2019;11(7):1-15. doi:10.3390/cancers11070946
- 474 12. Kramer M, Scholz M. Treatment planning for heavy-ion radiotherapy: Calculation and
475 optimization of biologically effective dose. *Phys Med Biol.* 2000;45(11):3319-3330.
476 doi:10.1088/0031-9155/45/11/314
- 477 13. Horcicka M, Meyer C, Buschbacher A, Durante M, Krämer M. Algorithms for the
478 optimization of RBE-weighted dose in particle therapy. *Phys Med Biol.* 2013;58(2):275-
479 286. doi:10.1088/0031-9155/58/2/275
- 480 14. Sørensen BS, Pawelke J, Bauer J, et al. Does the uncertainty in relative biological
481 effectiveness affect patient treatment in proton therapy? *Radiother Oncol.* 2021;163:177-
482 184. doi:10.1016/j.radonc.2021.08.016
- 483 15. McNamara AL, Schuemann J, Paganetti H. A phenomenological relative biological
484 effectiveness (RBE) model for proton therapy based on all published in vitro cell survival
485 data. *Phys Med Biol.* 2015;60(21):8399-8416. doi:10.1088/0031-9155/60/21/8399
- 486 16. Wedenberg M, Lind BK, Hårdemark B. A model for the relative biological effectiveness
487 of protons: The tissue specific parameter α/β of photons is a predictor for the sensitivity to
488 LET changes. *Acta Oncol (Madr).* 2013;52(3):580-588.

- 489 doi:10.3109/0284186X.2012.705892
- 490 17. Carabe A, Moteabbed M, Depauw N, Schuemann J, Paganetti H. Range uncertainty in
491 proton therapy due to variable biological effectiveness. *Phys Med Biol*. 2012;57(5):1159-
492 1172. doi:10.1088/0031-9155/57/5/1159
- 493 18. Frese MC, Yu VK, Stewart RD, Carlson DJ. A mechanism-based approach to predict the
494 relative biological effectiveness of protons and carbon ions in radiation therapy. *Int J*
495 *Radiat Oncol Biol Phys*. 2012;83(1):442-450. doi:10.1016/j.ijrobp.2011.06.1983
- 496 19. Hawkins RB. The relationship between the sensitivity of cells to high-energy photons and
497 the RBE of particle radiation used in radiotherapy. *Radiat Res*. 2009;172(6):761-776.
498 doi:10.1667/RR1655.1
- 499 20. Guan F, Peeler C, Bronk L, et al. Analysis of the track- and dose-averaged LET and LET
500 spectra in proton therapy using the geant 4 Monte Carlo code. *Med Phys*.
501 2015;42(11):6234-6247. doi:10.1118/1.4932217
- 502 21. Wilkens JJ, Oelfke U. Optimization of radiobiological effects in intensity modulated
503 proton therapy. *Med Phys*. 2005;32(2):455-465. doi:10.1118/1.1851925
- 504 22. Niemierko A, Schuemann J, Niyazi M, et al. Brain Necrosis in Adult Patients After Proton
505 Therapy: Is There Evidence for Dependency on Linear Energy Transfer? *Int J Radiat*
506 *Oncol Biol Phys*. 2021;109(1):109-119. doi:10.1016/j.ijrobp.2020.08.058
- 507 23. Garbacz M, Cordoni FG, Durante M, et al. Study of relationship between dose, LET and
508 the risk of brain necrosis after proton therapy for skull base tumors. *Radiother Oncol*.
509 2021;163:143-149. doi:10.1016/j.radonc.2021.08.015
- 510 24. Unkelbach J, Botas P, Giantsoudi D, Gorissen BL, Paganetti H. Reoptimization of
511 intensity modulated proton therapy plans based on linear energy transfer. *Int J Radiat*

- 512 *Oncol Biol Phys.* 2016;96(5):1097-1106. doi:10.1016/j.ijrobp.2016.08.038
- 513 25. Cao W, Khabazian A, Yepes PP, et al. Linear energy transfer incorporated intensity
514 modulated proton therapy optimization. *Phys Med Biol.* 2018;63(1):aa9a2e.
515 doi:10.1088/1361-6560/aa9a2e
- 516 26. Inaniwa T, Kanematsu N, Noda K, Kamada T. Treatment planning of intensity modulated
517 composite particle therapy with dose and linear energy transfer optimization. *Phys Med
518 Biol.* 2017;62(12):5180-5197. doi:10.1088/1361-6560/aa68d7
- 519 27. Traneus E, Ödén J. Introducing proton track-end objectives in intensity modulated proton
520 therapy optimization to reduce linear energy transfer and relative biological effectiveness
521 in critical structures. *Int J Radiat Oncol Biol Phys.* 2019;103(3):747-757.
522 doi:10.1016/j.ijrobp.2018.10.031
- 523 28. Gu W, Ruan D, Zou W, Dong L, Sheng K. Linear energy transfer weighted beam
524 orientation optimization for intensity-modulated proton therapy. *Med Phys.*
525 2021;48(1):57-70. doi:10.1002/mp.14329
- 526 29. An Y, Shan J, Patel SH, et al. Robust intensity-modulated proton therapy to reduce high
527 linear energy transfer in organs at risk: *Med Phys.* 2017;44(12):6138-6147.
528 doi:10.1002/mp.12610
- 529 30. Wieser HP, Cisternas E, Wahl N, et al. Development of the open-source dose calculation
530 and optimization toolkit matRad. *Med Phys.* 2017;44(6):2556-2568.
531 doi:10.1002/mp.12251
- 532 31. Bortfeld T, Schlegel W, Rhein B. Decomposition of pencil beam kernels for fast dose
533 calculations in three-dimensional treatment planning. *Med Phys.* 1993;20(2):311-318.
534 doi:10.1118/1.597070

- 535 32. Wilkens JJ, Oelfke U. Analytical linear energy transfer calculations for proton therapy.
536 *Med Phys.* 2003;30(5):806-815. doi:10.1118/1.1567852
- 537 33. Gu W, Ruan D, O'Connor D, et al. Robust optimization for intensity-modulated proton
538 therapy with soft spot sensitivity regularization. *Med Phys.* 2019;46(3):1408-1425.
539 doi:10.1002/mp.13344
- 540 34. Wächter A, Biegler LT. On the implementation of an interior-point filter line-search
541 algorithm for large-scale nonlinear programming. *Math Program.* 2006;106(1):25-57.
542 doi:10.1007/s10107-004-0559-y
- 543 35. Indelicato DJ, Ioakeim-Ioannidou M, Bradley JA, et al. Proton Therapy for Pediatric
544 Ependymoma: Mature Results From a Bicentric Study. *Int J Radiat Oncol Biol Phys.*
545 2021;110(3):815-820. doi:10.1016/j.ijrobp.2021.01.027
- 546 36. Niemierko A. Reporting and analyzing dose distributions: A concept of equivalent
547 uniform dose. *Med Phys.* 1997;24(1):103-110. doi:10.1118/1.598063
- 548 37. Niemierko A. A generalized concept of equivalent uniform dose (EUD). *Med Phys.*
549 1999;26(Abstract):1100.
- 550 38. Bai X, Lim G, Grosshans D, Mohan R, Cao W. Robust optimization to reduce the impact
551 of biological effect variation from physical uncertainties in intensity-modulated proton
552 therapy. *Phys Med Biol.* 2019;64(2). doi:10.1088/1361-6560/aaf5e9
- 553 39. Bai X, Lim G, Grosshans D, Mohan R, Cao W. A biological effect-guided optimization
554 approach using beam distal-edge avoidance for intensity-modulated proton therapy. *Med*
555 *Phys.* Published online 2020. doi:10.1002/mp.14335
- 556 40. Wu Q, Mohan R, Niemierko A, Schmidt-Ullrich R. Optimization of intensity-modulated
557 radiotherapy plans based on the equivalent uniform dose. *Int J Radiat Oncol Biol Phys.*

- 558 2002;52(1):224-235. doi:10.1016/S0360-3016(01)02585-8
- 559 41. Wu Q, Djajaputra D, Liu HH, Dong L, Mohan R, Wu Y. Dose sculpting with generalized
560 equivalent uniform dose. *Med Phys*. 2005;32(5):1387-1396. doi:10.1118/1.1897464
- 561 42. Allen Li X, Alber M, Deasy JO, et al. The use and QA of biologically related models for
562 treatment planning: Short report of the TG-166 of the therapy physics committee of the
563 AAPM. *Med Phys*. 2012;39(3):1386-1409. doi:10.1118/1.3685447
- 564 43. Hahn C, Heuchel L, Ödén J, et al. Comparing biological effectiveness guided plan
565 optimization strategies for cranial proton therapy: potential and challenges. *Radiat Oncol*.
566 2022;17(1):169. doi:10.1186/s13014-022-02143-x
- 567 44. Liu C, Patel SH, Shan J, et al. Robust optimization for intensity modulated proton therapy
568 to redistribute high linear energy transfer from nearby critical organs to tumors in head
569 and neck cancer. *Int J Radiat Oncol Biol Phys*. 2020;107(1):181-193.
570 doi:10.1016/j.ijrobp.2020.01.013
- 571 45. Giantsoudi D, Grassberger C, Craft D, Niemierko A, Trofimov A, Paganetti H. Linear
572 energy transfer-guided optimization in intensity modulated proton therapy: feasibility
573 study and clinical potential. *Int J Radiat Oncol Biol Phys*. 2013;87(1):216-222.
574 doi:10.1016/j.ijrobp.2013.05.013
- 575 46. Wilkens JJ, Oelfke U. A phenomenological model for the relative biological effectiveness
576 in therapeutic proton beams. *Phys Med Biol*. 2004;49(13):2811-2825. doi:10.1088/0031-
577 9155/49/13/004
- 578 47. Giovannini G, Böhlen T, Cabal G, et al. Variable RBE in proton therapy: Comparison of
579 different model predictions and their influence on clinical-like scenarios. *Radiat Oncol*.
580 2016;11(1):1-16. doi:10.1186/s13014-016-0642-6

- 581 48. Carabe-Fernandez A, Dale RG, Jones B. The incorporation of the concept of minimum
582 RBE (RBE_{min}) into the linear-quadratic model and the potential for improved
583 radiobiological analysis of high-LET treatments. *Int J Radiat Biol.* 2007;83(1):27-39.
584 doi:10.1080/09553000601087176
- 585 49. Friedrich T, Scholz U, Elssser T, Durante M, Scholz M. Calculation of the biological
586 effects of ion beams based on the microscopic spatial damage distribution pattern. *Int J*
587 *Radiat Biol.* 2012;88(1-2):103-107. doi:10.3109/09553002.2011.611213
- 588 50. Hirayama S, Matsuura T, Yasuda K, et al. Difference in LET-based biological doses
589 between IMPT optimization techniques: Robust and PTV-based optimizations. *J Appl Clin*
590 *Med Phys.* 2020;21(4):42-50. doi:10.1002/acm2.12844
- 591 51. Unkelbach J, Paganetti H. Robust Proton Treatment Planning: Physical and Biological
592 Optimization. *Semin Radiat Oncol.* 2018;28(2):88-96.
593 doi:10.1016/j.semradonc.2017.11.005
- 594 52. Wuyckens S, Saint-Guillain M, Janssens G, et al. Treatment planning in arc proton
595 therapy: Comparison of several optimization problem statements and their corresponding
596 solvers. *Comput Biol Med.* 2022;148(February):105609.
597 doi:10.1016/j.combiomed.2022.105609
- 598 53. Toussaint L, Indelicato DJ, Holgersen KS, et al. Towards proton arc therapy: physical and
599 biologically equivalent doses with increasing number of beams in pediatric brain
600 irradiation. *Acta Oncol (Madr).* 2019;58(10):1451-1456.
601 doi:10.1080/0284186X.2019.1639823

602 **Appendix**603 Tables 1-3 list the mean and max LET_d values in target and OARs from ConstRBEopt, LETopt,

604 VarRBEopt, and hRBEopt plans for all cases.

605 Table 1. LET_d (keV/um) values for target.

Case	ConstRBEopt		LETopt		VarRBEopt		hRBEopt	
	Mean	Max	Mean	Max	Mean	Max	Mean	Max
1	4.44	6.81	5.62	8.11	4.62	6.20	4.58	6.69
2	3.92	8.03	4.06	7.46	3.89	7.42	3.71	7.50
3	4.05	5.96	5.26	7.14	4.22	5.91	3.93	5.98
4	3.87	6.15	4.65	7.06	3.72	5.98	3.74	6.39
5	3.82	6.96	4.11	7.09	3.77	6.75	3.72	6.78
6	4.27	6.90	5.30	7.25	4.15	6.65	4.00	6.71
7	4.01	6.66	5.26	7.29	4.05	6.20	3.91	6.57
8	4.15	9.83	4.98	8.56	4.19	8.31	4.07	8.41
9	4.01	7.44	4.39	6.40	4.04	6.04	3.97	6.33
10	4.10	7.41	4.85	7.06	4.00	7.93	4.07	7.37

606

607 Table 2. LET_d (keV/um) values for brainstem.

Case	ConstRBEopt		LETopt		VarRBEopt		hRBEopt	
	Mean	Max	Mean	Max	Mean	Max	Mean	Max
1	4.34	10.40	3.48	9.51	3.79	7.90	4.09	9.17
2	4.45	7.13	3.24	5.64	3.69	5.97	3.12	6.87
3	2.64	6.28	2.30	6.48	2.34	5.61	2.02	6.02

4	3.59	6.02	2.99	6.07	3.25	6.08	3.03	5.92
5	1.91	6.00	1.83	6.05	1.81	5.79	1.71	5.76
6	3.49	7.78	2.72	6.51	2.98	6.42	2.32	7.34
7	3.42	13.54	2.51	12.51	3.13	11.65	3.02	13.09
8	2.69	10.83	2.52	9.35	2.52	8.93	2.39	11.49
9	2.03	8.27	1.73	8.33	2.05	7.10	1.98	7.27
10	2.61	6.42	2.62	5.98	2.63	6.05	2.55	5.52

608

609 Table 3. LET_d (keV/um) values for spinal cord.

Case	ConstRBEopt		LETopt		VarRBEopt		hRBEopt	
	Mean	Max	Mean	Max	Mean	Max	Mean	Max
1	2.64	7.15	2.19	6.52	2.26	6.65	2.62	6.92
2	0.94	9.10	0.72	8.05	0.80	7.82	0.91	10.96
3	0.26	5.16	0.24	5.32	0.23	4.55	0.21	4.04
4	0.58	7.82	0.40	5.02	0.42	5.60	0.29	4.06
5	2.46	7.87	1.71	6.12	1.53	4.64	1.39	5.25
6	0.41	8.05	0.33	6.35	0.34	6.62	0.37	7.98
7	1.95	7.45	1.29	5.01	1.53	5.67	1.17	4.97
8	4.10	13.73	2.70	9.38	2.87	9.07	2.63	9.10
9	0.93	11.63	0.72	9.13	0.81	9.10	0.76	9.66
10	2.05	11.38	1.78	7.84	1.46	9.98	1.46	10.18

610

611

612 Tables 4-6 summarize constant RBE-weighted dose for all cases.

613 Table 4. Mean dose (Gy(RBE)) in target based on constant RBE-weighted dose.

Case	ConstRBEopt	LET _{opt}	VarRBEopt	hRBEopt
1	55.79	56.27	53.55	56.12
2	56.66	56.71	54.34	56.31
3	56.27	56.43	53.99	56.02
4	55.66	55.71	53.47	54.89
5	56.1	56.22	54	56.48
6	55.87	56.43	53.28	56.98
7	55.51	55.94	53.34	55.42
8	56.02	55.37	53.6	56.62
9	56.32	56.81	53.77	56.47
10	56.07	56.37	53.20	56.25

614

615 Table 5. Mean and max dose (Gy(RBE)) in brainstem based on constant RBE-weighted dose.

Case	ConstRBEopt		LET _{opt}		VarRBEopt		hRBEopt	
	Mean	Max	Mean	Max	Mean	Max	Mean	Max
1	27.08	58.18	27.8	60	22.87	57.53	27.22	58.54
2	38.43	60.64	39.75	61.8	35.81	57.56	39.89	62.09
3	24.87	58.49	25.58	59.18	27.32	56.52	28.54	57.99
4	43.48	57.74	46.77	58.32	43.42	55.31	44.32	56.69
5	27.85	61.72	27.75	60.38	24.94	57.2	24.45	58.96
6	25.07	59.3	28.6	61.03	24.09	55.76	22.94	60.16
7	17.9	57.41	23.84	58.09	17.49	55.18	19.79	56.95

8	22.18	59.81	22.44	60.46	19.22	56.56	20.17	59.59
9	20.36	59.97	19.95	61.96	18.65	57.07	19.50	59.71
10	31.41	58.07	32.19	59.30	29.11	56.27	31.4	58.54

616

617 Table 6. Mean and max dose (Gy(RBE)) in spinal cord based on constant RBE-weighted dose.

Case	ConstRBEopt		LETopt		VarRBEopt		hRBEopt	
	Mean	Max	Mean	Max	Mean	Max	Mean	Max
1	8.48	43.66	8.1	44.17	6.54	37.19	8.33	44.07
2	2.55	36.56	2.55	36.28	2.30	31.26	2.42	36.08
3	1.58	53.53	1.69	53.95	1.71	53.07	1.72	54.98
4	2.26	52.78	2.33	52.4	2.24	48.78	2.17	50.58
5	12.54	55.24	13.16	54.45	14.27	53.07	14.15	54.94
6	0.94	40.57	0.94	40.01	0.84	35.21	0.83	38.46
7	6.16	49.71	5.24	45.44	5.17	42.82	5.72	47.15
8	9.34	56.87	10.71	55.37	9.16	49.89	11.8	57.61
9	2.78	52.78	3.59	55.84	3.33	51.07	3.36	54.66
10	6.08	49.63	7.14	50.56	5.20	47.19	5.69	50.42

618

619

620 Tables 7-9 summarize variable RBE-weighted dose for all cases.

621 Table 7. Mean dose (Gy(RBE)) in target based on variable RBE-weighted dose.

Case	ConstRBEopt	LETopt	VarRBEopt	hRBEopt
1	58.15	60.03	56.1	58.72
2	58.55	58.77	56.16	57.93
3	58.46	60.13	56.33	58.07
4	57.15	58.11	54.78	56.24
5	57.85	58.34	55.66	58.11
6	58.18	60.04	55.4	59
7	57.37	59.31	55.22	57.18
8	58.28	59.6	55.87	58.81
9	58.17	59.11	55.59	58.25
10	58.24	59.47	56.38	58.38

622

623 Table 8. Mean and max dose (Gy(RBE)) in brainstem based on variable RBE-weighted dose.

Case	ConstRBEopt		LETopt		VarRBEopt		hRBEopt	
	Mean	Max	Mean	Max	Mean	Max	Mean	Max
1	32.76	68.78	32.13	65.98	27.43	59.41	32.64	67.11
2	45.43	67.43	44.47	68.48	41.21	63.77	44.39	69.26
3	28.93	67.84	28.95	69.70	30.86	64.03	31.54	64.41
4	47.63	65.27	49.44	64.24	46.97	62.08	47.46	63.62
5	31.14	70.68	30.85	69.95	27.87	64.72	27.21	66.38
6	30.23	66.75	32.67	69.33	28.31	62.9	25.96	62.02
7	22.56	67.75	27.35	66.1	21.69	63.36	23.97	66.5

8	26.12	70.7	26.14	68.61	22.73	62.25	20.29	66.31
9	22.75	69.4	21.82	65.62	20.99	61.1	21.79	65.44
10	35.7	66.72	36.39	69.45	33.02	63.58	35.4	66.06

624

625 Table 9. Mean and max dose (Gy(RBE)) in spinal cord based on variable RBE-weighted dose.

Case	ConstRBEopt		LETopt		VarRBEopt		hRBEopt	
	Mean	Max	Mean	Max	Mean	Max	Mean	Max
1	11.88	54.59	10.86	53.84	9.29	47.15	11.79	55.67
2	3.78	48.06	3.51	45.08	3.31	41.42	3.57	45.55
3	1.95	59.17	2.04	60.35	2.04	57.00	2.02	59.09
4	3.03	56.49	2.88	55.79	2.81	52.3	2.53	52.09
5	15.87	60.31	15.47	55.84	16.26	54.92	15.96	56.08
6	1.42	54.87	1.34	51.95	1.22	46.87	1.25	51.66
7	8.57	58.28	6.81	51.47	6.99	49.66	7.09	51.97
8	14.63	72.72	14.45	63.07	12.88	58.8	14.99	65.17
9	4.09	62.32	4.61	61.61	4.46	59.1	4.44	60.46
10	8.85	58.85	9.72	58.40	7.01	50.89	7.6	55.52

626

627

628 Table 10. $\Delta\text{EUD}_{\text{VOI}}$ and ΔEUD (in Gy(RBE)) based on variable RBE \times Dose for 10 ependymoma
 629 cases.

Case #	ΔEUD LET _{opt} – ConstRBE _{opt}				ΔEUD VarRBE _{opt} – ConstRBE _{opt}				ΔEUD hRBE _{opt} – ConstRBE _{opt}			
	CTV	BS	Cord	Total	CTV	BS	Cord	Total	CTV	BS	Cord	Total
1	2.21	-1.03	-1.17	4.41	-1.91	-6.22	-5.58	9.89	1.04	0.24	0.62	0.18
2	0.18	-1.82	-1.33	3.33	-2.57	-4.76	-3.71	5.9	-0.57	-1.68	-1.23	2.34
3	1.57	-0.01	1.12	0.46	-2.13	-2.02	-0.18	0.07	-0.4	-1.05	0.28	0.37
4	0.89	0.2	-0.55	1.24	-2.33	-1.94	-2.27	1.88	-0.91	-1.53	-2.62	3.24
5	0.49	-0.63	-1.71	2.83	-2.15	-4.02	-1.01	2.88	0.28	-4.48	-1.5	6.26
6	1.7	1.14	-1.36	1.92	-2.88	-1.68	-3.92	2.72	0.49	-2.01	-1.67	4.17
7	1.78	0	-4.73	6.51	-2.22	-3.37	-5.64	6.79	-0.2	1.07	-3.86	2.59
8	1.18	-0.14	-2.85	4.17	-3	-5.56	-6.21	8.77	0.54	-3.27	-1.42	5.23
9	0.8	-0.43	1.15	0.08	-2.59	-2.55	-0.23	0.19	0.09	-0.55	0.24	0.4
10	1.13	0.39	0.6	0.14	-3.05	-2.81	-4.54	4.3	0.11	-0.31	-1.89	2.31
Mean	1.193	-0.233	-1.083	2.509	-2.483	-3.493	-3.329	4.339	0.047	-1.357	-1.305	2.709

630

631

632

633 Table 11. Δ EU based on constant RBE-weighted dose for all cases.

Case #	Δ EU				Δ EU				Δ EU			
	LET _{opt} - ConstRBE _{opt}				VarRBE _{opt} - ConstRBE _{opt}				hRBE _{opt} - ConstRBE _{opt}			
	CTV	BS	Cord	Total	CTV	BS	Cord	Total	CTV	BS	Cord	Total
1	0.56	-0.08	-0.4	1.04	-3.31	-5.45	-5.06	7.2	0.34	-0.03	-0.07	0.44
2	0.18	0.58	0.28	-0.68	-2.73	-3.15	-2.81	3.23	-0.01	1.09	-0.26	-0.84
3	0.01	-0.03	0.7	-0.66	-2.48	-1.61	0.09	-0.96	-0.19	0.32	1.17	-1.68
4	0.01	0.97	0.57	-1.53	-2.23	-1.52	-1.21	0.5	-0.73	-0.54	-0.33	0.14
5	0.06	-0.28	-0.17	0.51	-2.47	-3.36	0.88	0.01	0.25	-3.53	0.95	2.83
6	0.27	1.94	-0.43	-1.24	-3.36	1.79	-2.68	-2.47	0.46	3.39	-1.14	-1.79
7	0.21	1.99	-2.93	1.15	-2.61	-2.66	-4.46	4.51	-0.09	4.02	-1.43	-2.68
8	-0.02	0.04	1.23	-1.29	-7.38	-4.71	-1.81	-0.86	0.83	-2.65	2.51	0.97
9	0.45	0.34	3.75	-3.64	-2.66	-2.35	1.3	-1.61	0.29	-0.2	2.43	-1.94
10	0.19	0.01	1.02	-0.84	-1.91	-1.18	-1.52	0.79	0.09	0.07	0.14	-0.12
Mean	0.192	0.548	0.362	-0.718	-3.114	-2.42	-1.728	1.034	0.095	0.214	0.154	-0.273

634